Driveline Backlash and Half-shaft Torque Estimation for Electric Powertrains Control

# BACKLASH AND HALF-SHAFT TORQUE ESTIMATION FOR ELECTRIC POWERTRAINS CONTROL

Guido Ricardo Guercioni[1], Enrico Galvagno[1], Antonio Tota[1], Alessandro Vigliani[1] and Tong Zhao[2]

[1]Dipartimento di Ingegneria Meccanica e Aerospaziale - Politecnico di Torino; [2]The Ohio State University

*Citation*: Guercioni, G.R., Galvagno, E., Tota, A., Vigliani, A. et al., "Driveline Backlash and Half-shaft Torque Estimation for Electric Powertrains Control," SAE Technical Paper 2018-01-1345, 2018, doi:10.4271/2018-01-1345.

## Abstract

The nonlinear behavior of automotive powertrains is mainly due to the presence of backlash between engaging components. In particular, during tip-in or tip-out maneuvers, backlash allows the generation of impacts that negatively affect the vehicle NVH performance. Due to the faster response of electric motors with respect to conventional internal combustion engines, this problem is even more critical for electric vehicles. In order to employ numerical optimal control methods for backlash compensation, the system states have to be known. In this paper, an electric powertrain is modeled as a two-mass oscillator with lumped backlash. This model estimates the system states when in no-contact mode while a Kalman filter that relies only on commonly available speed measurements is active in the contact phase. The powertrain model is validated using experimental data collected during vehicle testing and the online estimated half-shaft torque is shown. In addition, simulations are performed to illustrate that the system states can be properly determined with the proposed estimator.

## Introduction

Over the past decade, the automotive industry has experienced an increasing demand for improved NVH (Noise Vibration and Harness) performance.

The nonlinear behavior of transmission systems is mainly due to the presence of backlash between engaging components, e.g. gears. Backlash allows the generation of impacts (impulsive forces), causing noise and vibration issues [1].

Typical maneuvers during which nonlinear transient vibrations can be excited are those that, in some way, determine a change in the active contact flank of the driveline linkages. For example, throttle tip-in/tip-out generate a torque transient that may produce a disturbance to vehicle occupants [2]. During these maneuvers, the driveline backlash is traversed and no torque is transmitted to the wheels until contact is achieved again. The impact at the time driveline components re-engage causes a sudden large variation of the half-shaft torque which, together with the powertrain flexibility, generates driveline oscillations, i.e., an initial jerk of the vehicle (referred to as shunt) preceding shuffle oscillations [3], [4].

The development of advanced magnetic materials, power electronics, and digital control systems has led to the integration of EMs (Electric Machines) in automotive powertrains to supply for the need of improved fuel consumption and reduced air pollutant emissions [5], [6].

EMs present a short time lag between the torque request and the actual torque output [3]. The response delay of conventional ICEs (Internal Combustion Engines) and the EMs used in automotive applications is significantly different. The later show a shorter time lag to meet a certain torque request [7], [8].

Due to the faster response of electric motors with respect to conventional ICEs, the need to mitigate the negative effects of powertrain backlash and flexibility on drivability is even more critical for EVs (Electric Vehicles) [4].

To compensate for these problems, proper control is needed. However, high-performance controllers for backlash compensation require high-quality measurements of the current state of the powertrain [9], [10]. The cost and capabilities of current available sensors made the position within the backlash region and the half-shafts torque not available as inputs for powertrain control algorithms [11]. As a result, several estimators have been proposed in literature.

In [12] a nonlinear observer based on extended Kalman filter theory for backlash gap position estimation is developed and the experimental validation is presented in [13]. Instead, in [9] experimentally validated backlash state and size estimators for rotating systems are described. The estimators are based on switched Kalman filters. Unfortunately, the proposed approaches require measurements of the angular position of the engine crankshaft and the wheels, which are typically unavailable in commercial vehicles.

This paper proposes a model-based nonlinear observer that is designed to estimate the system states. The estimator requires as inputs only speed measurements of the EM output shaft and the wheels which are commonly available in production vehicles.

The estimator is based upon a switching structure that combines a Kalman Filter and a control-oriented model of the powertrain. The model estimates the system states when in no-contact mode while the Kalman filter is active in the contact phase.

The electric powertrain is modeled as a two-mass oscillator with lumped backlash. A validation of the model is performed using experimental data collected during vehicle testing. The results showed that the model can properly simulate the nonlinear behavior of the powertrain while being simple enough to be suitable for online implementation and control design.

A similar estimator is proposed in [11], [14], [15] for drivability control of a conventional vehicle. Here, the powertrain model is adapted to the EV of interest. As stated before, the response of an EM is much faster than that of an ICE, in addition, regenerative braking torque is usually larger than the ICE braking torque in a conventional car, which results in more severe oscillations [4]. For this reason, a detailed validation of the EM speed right after the tip-in/tip-out events

is conducted. Insides on the frequency content of the mentioned vibrations are also provided.

Due to the mentioned characteristics of full-electric powertrains, high precision on the system states estimates is required if an observer is meant to be used for drivability control. Furthermore, even if not discussed here, the interaction of these algorithms with other systems as the ESC (Electronic Stability Control) should be carefully addressed since requests to the same actuators may be generated by different powertrain controllers, e.g. ICE/EM and mechanical brakes [16], [17]. In this work, an assessment on the quality of the predicted state transitions is presented and the effect of the input sampling frequency is explored.

The present paper is organized as follows. First, the electric drivetrain layout of interest is described together with the mathematical formulation of the developed control-oriented model. Next, the powertrain model is validated using experimental data collected during vehicle testing. Then, the estimator design is presented and the online estimated half-shaft torque obtained with a simplified version of the estimator is shown and analyzed. Finally, simulations are performed to illustrate that the system states can be properly determined with the proposed estimator.

## Powertrain description and modeling

### *Powertrain description*

The electric powertrain of interest is depicted in Figure 1. The powertrain consists of an EM, a mechanical coupler, a differential and the half-shafts. The EM is connected to the driveshaft through a mechanical coupler. A single gear ratio is available to the electric motor. The main contributions to the total driveline backlash come from the constant-velocity (CV) joints, the mechanical coupler and the differential.

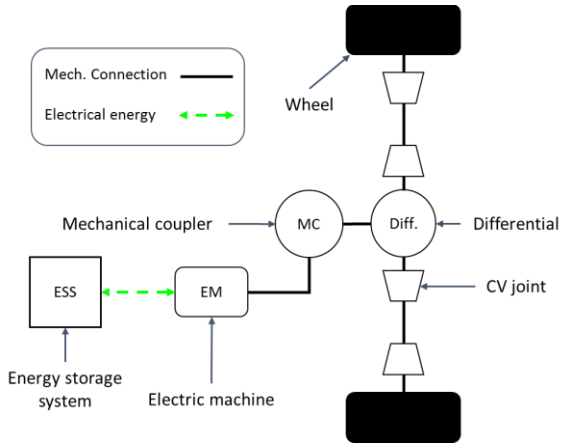


Figure 1. Powertrain layout.

### *Control-oriented model*

A control-oriented model of the powertrain is developed.

The model used for the estimator must be able to deal with the change in the number of the driveline kinematic DOF (Degrees Of Freedom) due to the presence of backlash in the system. Furthermore, the model should properly account for the main powertrain components compliance and damping. Another requirement is that the complexity of the model has to make it suitable for online implementation.

The electric powertrain is modeled as a two-mass oscillator with lumped backlash as seen in Figure 2.

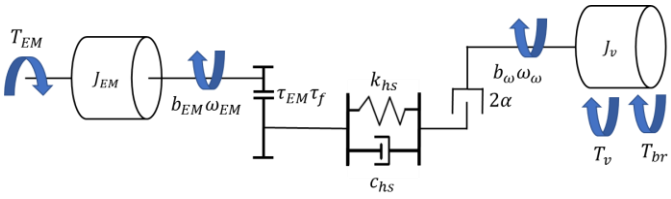


Figure 2. Powertrain model.

One inertia represents the EM, the other corresponds to the load (wheels and vehicle). The inertias of the remaining powertrain components are lumped with the one of the EM.

The dynamics of the EM is described by:

$$J_{EM}\dot{\omega}_{EM}(t) = T_{EM}(t) - \frac{T_{hs}(t)}{\tau_{EM}\tau_f} - b_{EM}\omega_{EM}(t) \quad (1)$$

where $J_{EM}$ is the EM inertia, $b_{EM}$ is the viscous friction coefficient associated to the EM, $\tau_f$ is the final drive ratio, $\tau_{EM}$ is the transmission ratio introduced by the mechanical coupler and $T_{hs}$ is the shaft torque.

The backlash contributions throughout the driveline are lumped together into one single backlash as in [4], [14], [18]. This is a reasonable approximation, if the rotating masses between the backlashes are negligible [9].

A flexible shaft with backlash connects the EM and the load inertia. The shaft torque is computed using the physical modeling approach described in [19].

The torque exchanged between engaging components is computed according to:

$$T_{hs}(t) = k_{hs}(\theta_d(t) - \theta_b(t)) + c_{hs}(\omega_d(t) - \omega_b(t)) \quad (2)$$

where $k_{hs}$ and $c_{hs}$ are the equivalent stiffness and damping coefficients. $\theta_d$ and $\omega_d$ are, respectively, the total shaft displacement angle and rate. $\theta_b$ is the position within the backlash gap and $\omega_b$ refers to the speed at which it is being traversed.

As shown in [20], the main powertrain flexibility is in the half-shafts, hence including them in the model as a damped torsional flexibility allows it to describe the main oscillations of the driveline.

The total shaft displacement is calculated as:

$$\theta_d(t) = \frac{\theta_{EM}(t)}{\tau_{EM}\tau_f} - \theta_\omega(t) \quad (3)$$

where $\theta_\omega$ is the angular position of the vehicle wheels. Note that for simplicity, the motion of the right and left wheel on the same axle is considered to be equal.

The nonlinear model for the backlash position gives:

$$\omega_b(t) = \begin{cases} \max\left(0, \omega_d(t) + \frac{k_{hs}}{c_{hs}}(\theta_d(t) - \theta_b(t))\right) & \theta_b(t) = -\alpha \\ \omega_d(t) + \frac{k_{hs}}{c_{hs}}(\theta_d(t) - \theta_b(t)) & |\theta_b(t)| < \alpha \\ \min\left(0, \omega_d(t) + \frac{k_{hs}}{c_{hs}}(\theta_d(t) - \theta_b(t))\right) & \theta_b(t) = \alpha \end{cases} \quad (4)$$

The previous equation implies that the backlash angular position can only change within the length of the backlash gap (2α). Furthermore, according to this equation, the powertrain has three operating modes:

- Contact on the drive side: $\theta_b(t) = \alpha$
- Contact on the coast side: $\theta_b(t) = -\alpha$
- No-contact: $|\theta_b(t)| < \alpha$

For an EV, if we define the contact as being on the drive side when half-shafts are transmitting a driving torque, then the contact during regenerative deceleration is on the coast side [4]. According to equation 4, when in contact mode on either side, the total shaft displacement rate must be large enough in relation to the shaft twist in order to start traversing the backlash region.

As explained in [19], equations 2 and 4 imply that when inside the backlash gap there is no torque being transmitted through the shaft.

The dynamic equation for the second DOF is:

$$J_v\dot{\omega}_\omega(t) = T_{hs}(t) - T_v(t) - T_{br}(t) - b_\omega\omega_\omega(t) \quad (5)$$

where $J_v$ is the vehicle equivalent inertia, $b_\omega$ is the viscous friction coefficient and $T_{br}$ is the total torque applied by the mechanical brakes.

The vehicle load $T_v$ is the sum of three contributions: tire rolling resistance $T_{rr}$, aerodynamic drag $T_{aer}$ and road grade $T_g$.

$$T_v(t) = T_{rr}(t) + T_{aer}(t) + T_g(t) \quad (6)$$

$$T_{aer}(t) = a_{0,aer}\omega_\omega^2(t) \quad (7)$$

$$T_{rr}(t) = mg\left(a_{0,rr} + a_{1,rr}\omega_\omega(t) + a_{2,rr}\omega_\omega^2(t)\right) \quad (8)$$

$$T_g(t) = mgr_w sin(\varphi) \quad (9)$$

where $a_{0,aer}$, $a_{0,rr}$, $a_{1,rr}$ and $a_{2,rr}$ are constant known coefficients. $m$ is the vehicle mass, $\varphi$ is the road slope angle and $r_w$ is the wheel radius.

## Powertrain model validation

The control-oriented model described in the previous section was built in MATLAB®/Simulink® environment and experimentally validated using data collected during vehicle testing. Tip-in/Tip-out maneuvers were used for the validation. The measured speed of the EM and the wheels (mean value on the driven axle) seen during the tests are compared to the simulated variables. The input to the model is torque request to the EM, the mechanical brakes were not employed.

Figure 3 shows a comparison of measured and simulated variables during a Tip-out test in which the torque request to the EM goes from 30 to -20 Nm. It can be seen that, in general, the model outputs match the experimental data well.

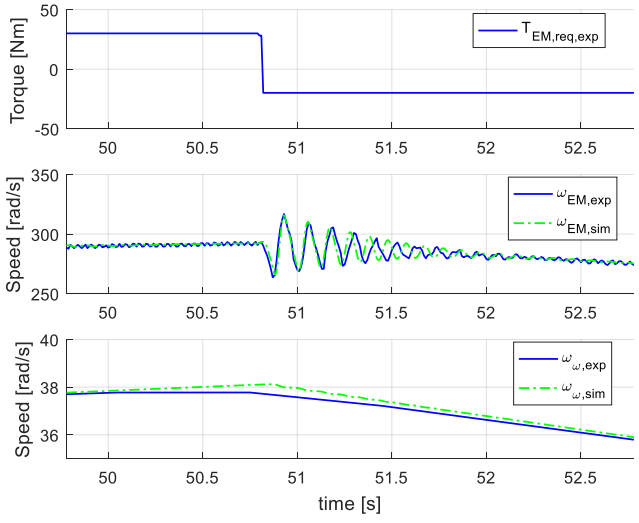


Figure 3. Model validation: tip-out.

The frequency of the simulated EM speed oscillations starts to differ from the experimental data approximately 1 s after the tip-out event.

Figure 4-a shows a spectrogram of the EM speed. It can be clearly seen that traversing the backlash region excites the nonlinearity of the system: the frequency of the oscillations increases with time. On the other hand, when the system is in contact mode, it behaves linearly as illustrated in Figure 4-b where a spectrogram of the EM speed after a torque step from -20 to -80 Nm is shown. It can be appreciated from these two figures that the frequency of the system after the tip-out converges to the value it has in contact mode.

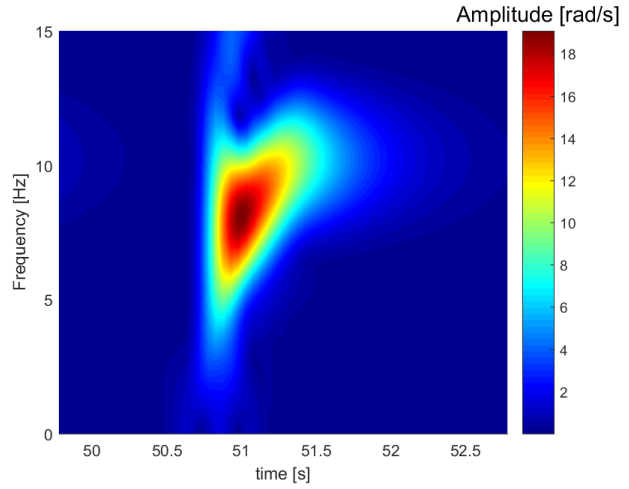


a) Backlash traversed

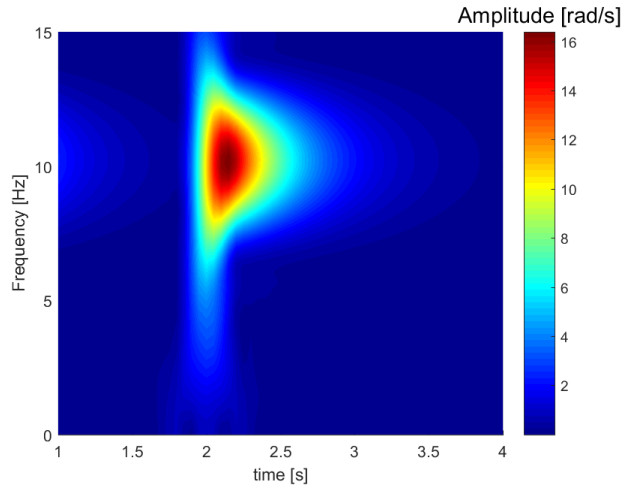


b) Contact preserved

Figure 4. EM speed frequency content.

Based on the previous observations, the equivalent stiffness and damping coefficients $k_{hs}$ and $c_{hs}$ are tuned to match the oscillations right after the tip-in/tip-out events. The first impacts generated have more associated energy and therefore are more critical in terms of vehicle drivability. For this reason, it is desirable to give the most accurate information possible to powertrain control strategies about the system state in these instances. Furthermore, after contact is achieved again, the Kalman filter can compensate for model inaccuracies using information from the measured variables.

Due to the relatively low sampling frequency of the acquisitions (100 Hz) and the number of teeth of the measuring gear, the computed wheel speed has to be filtered.

Figure 5 presents the model validation for a tip-in maneuver from -20 to 30 Nm. The same considerations made before still apply.

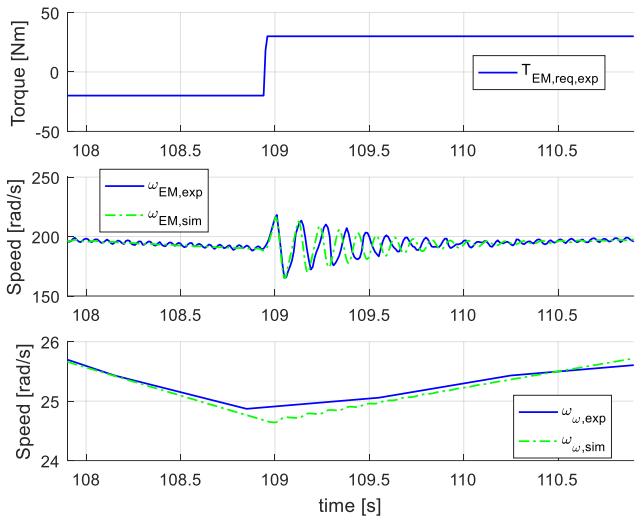


Figure 5. Model validation: tip-in.

## Estimator description

The designed estimator should be able to provide real-time information about the operating mode of the powertrain and other useful and often not measurable variables like the wheel torque, the total shaft displacement and the backlash angle to powertrain control algorithms for drivability improvement.

### *Powertrain operating mode transitions*

As explained in the previous sections, the powertrain is considered to have three operating modes: contact on the drive side, no-contact and contact on the coast side.

When the system enters the no-contact mode, the EM and the wheels are effectively decoupled and the system observability is lost [11], [14]. This could be solved by using angle measurements, but these signals are not usually available in production vehicles. This means that state information can only be estimated by a simulator in this mode [21], [22].

With these considerations in mind, an estimator, illustrated in Figure 6, is designed based upon a switching structure that combines a linear discrete-time Kalman Filter and a control-oriented model of the powertrain. Similar to [14], the model estimates the system states when in no-contact mode while the Kalman filter is active in the contact phase.

The inputs to the estimator are:

- EM speed: $\omega_{EM}$
- Mean driven wheels speed: $\omega_{\omega}$
- EM torque: $T_{EM}$
- Mechanical brakes torque: $T_{br}$

The estimated variables:

- Powertrain operating mode
- Backlash angular position and speed: $\theta_b$,$\omega_b$
- Total shaft angular displacement angle and speed: $\theta_d$,$\omega_d$
- Flexible shaft torque: $T_{hs}$

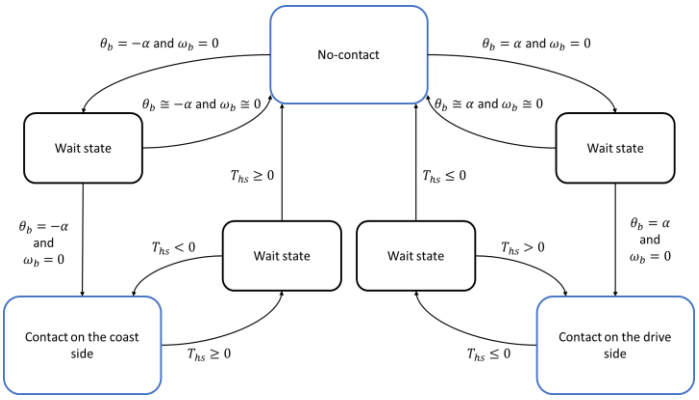


Figure 6. Estimator scheme.

The powertrain mode transitions are handled by a state machine created using Stateflow®.

The estimator is initialized assuming contact on the drive side. Figure 6 shows that in order to validate the transition to the no-contact mode the shaft torque estimated by the Kalman filter must be equal or lower than zero. As mentioned before, the Kalman filter is able to compensate for model uncertainties and measurement noise when making its estimates [23]. The measured data allows the filter to correct the deviations from the real behavior of the system that an open-loop model could present.

Instead, to go from the no-contact mode to the contact on the drive side mode, the backlash position must be equal to $\alpha$ and its rate of change equal to zero. The information regarding the backlash region traversal is provided by the control-oriented model previously described which is initialized using the Kalman filter estimates.

Analogous considerations are made for the transitions between the contact at the coast side mode and the no-contact mode.

Moreover, wait states are introduced to avoid chattering between modes. Basically, once the conditions for a mode switch are satisfied, it is required that they are fulfilled for a certain user-defined time before validating the transition.

### *Discrete-time Kalman filter*

A linear discrete-time Kalman filter is implemented as reported in [23].

#### System state space formulation in contact mode

In order to implement the Kalman filter it is necessary to linearize the powertrain model equations. Therefore, the aerodynamic friction and rolling resistance are linearized according to:

$$T_{aer}(t) = \left(b_{0,aer} + b_{1,aer} r_{\omega} \omega_{\omega}(t)\right) r_{\omega} \tag{10}$$

$$T_{rr}(t) = b_{0,rr} + b_{1,rr} \omega_{\omega}(t) \tag{11}$$

where $b_{0,aer}$, $b_{1,aer}$, $b_{0,rr}$ and $b_{1,rr}$ are constant known coefficients.

In the contact mode, the system can be described with the following state-space formulation:

$$\dot{x} = Ax + Bu + f$$

$$y = Cx \tag{12}$$

The state $x$ and input $u$ vectors are:

$$x = [\theta_d \quad \omega_{EM} \quad \omega_{\omega}] \;\; ; \;\; u = \begin{bmatrix} T_{EM} \\ T_{br} \end{bmatrix} \tag{13}$$

The rest of the matrices are presented for the contact on the drive side mode:

$$A = \begin{bmatrix} 0 & \frac{1}{\tau_{EM}\tau_f} & -1 \\ -\frac{k_{hs}}{J_{EM}\tau_{EM}\tau_f} & -\left(\frac{c_{hs}}{J_{EM}\tau_{EM}^2\tau_f^2} + \frac{b_{EM}}{J_{EM}}\right) & \frac{c_{hs}}{J_{EM}\tau_{EM}\tau_f} \\ \frac{k_{hs}}{J_v} & \frac{c_{hs}}{J_v\tau_{EM}\tau_f} & -\frac{c_{hs} + b_{1,rr} + r_\omega^2 b_{1,aer} + b_\omega}{J_v} \end{bmatrix}$$

$$B = \begin{bmatrix} 0 & 0 \\ \frac{1}{J_{EM}} & 0 \\ 0 & -\frac{1}{J_v} \end{bmatrix}$$

$$f = \begin{bmatrix} 0 & \frac{k_{hs}\theta_b}{J_{EM}\tau_{EM}\tau_f} & -\frac{k_{hs}\theta_b + b_{0,rr} + r_\omega b_{0,aer}}{J_v} \end{bmatrix}$$

$$C = \begin{bmatrix} 0 & 0 & 0 \\ 0 & 1 & 0 \\ 0 & 0 & 1 \end{bmatrix} \quad (14)$$

The backlash angle is considered as constant in either of the contact modes. The only difference between these two modes is the sign of the backlash angle.

Note that the presented model needs to be discretized to be implemented into the Kalman filter.

## Experimental results

The designed estimator was tested experimentally during the tip-in/tip-out maneuvers previously described.

### *Simplified estimator scheme*

Due to the characteristics of the experimental setup, the minimum time step at which the estimator could be implemented was 10 ms, coherently with the sampling frequency of the measured variables.

The control-oriented model is not able to run with this time-step. For this reason, the proposed estimator was simplified in order for it to be employed during vehicle testing.

The simplified version of the estimator is illustrated in Figure 7. Since the powertrain model cannot be used, the transition from the no-contact mode to either of the contact modes is given by the sign of the torque requested by the driver and a delay is introduced. The idea is to give enough time to the powertrain controller to stabilize the contact on one side according to the driver torque request.

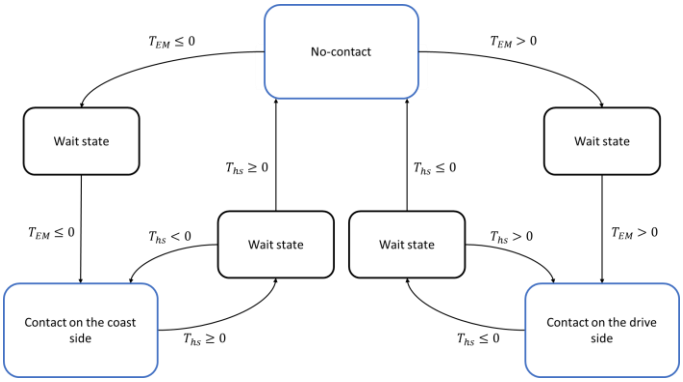


Figure 7. Simplified estimator scheme.

Figure 8 shows the estimates of the system states made by the Kalman filter during the same tip-out maneuver used for the model experimental validation. It can be seen that the value of the measured variables is well matched by the filter. For the shaft total displacement, only the estimate is shown since this variable is not an input to the filter.

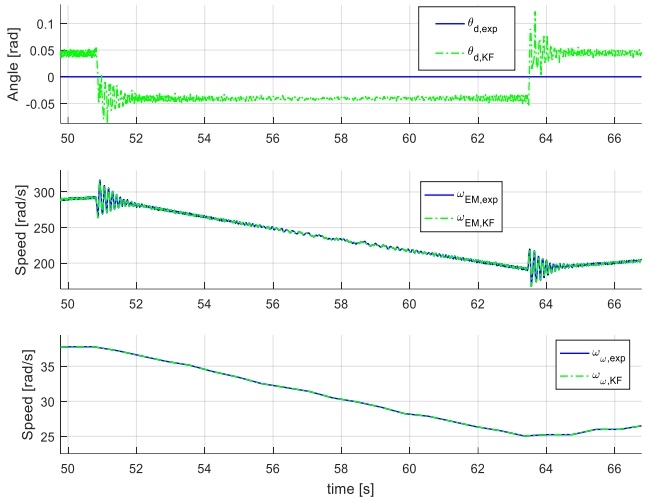


Figure 8. Kalman filter outputs: system states.

The estimate of the torque transmitted to the wheels is presented in Figure 9. Unfortunately, a measurement of the half-shaft torque was not available, so the experimentally validated powertrain model is employed to assess the quality of the estimate. It can be seen that, in general, the estimated torque matches properly its reference. It is important to consider that the state space formulation used for the Kalman filter is only valid during the contact modes.

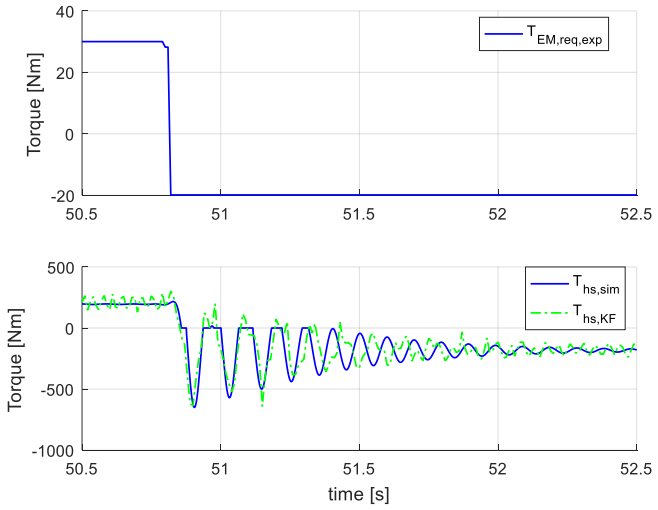


Figure 9. Kalman filter outputs: shaft torque.

Figure 10 allows to assess the quality of the mode transitions reported by the estimator. As for the half-shaft torque, the developed model is used as a reference. In the figure, the transition from contact to no-contact mode is indicated with a vertical dashed line. This transition depends directly on the wheel torque estimate sign. It can be appreciated that, because of the size of the time-step used, the traversing of the backlash region is reported around the time the impact on the opposite side happens. This would prevent control algorithms for backlash mitigation to properly modify the EM torque.

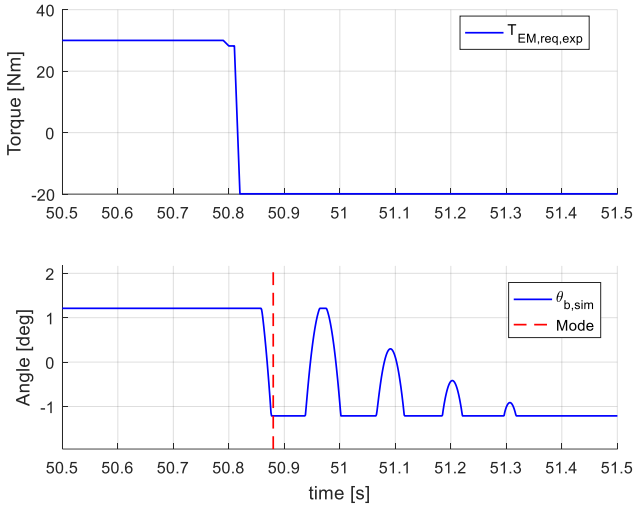


Figure 10. Mode transition verification.

## Simulation results

In this section, a series of simulations are undertaken to assess the potentialities of the proposed estimator.

The control-oriented model is able to run correctly with a time-step equal or higher than 1 ms, meaning that working with such step-size eliminates the need to simplify the designed estimator.

Figure 11 shows the observer estimates obtained with a step size of 1 ms and a sampling frequency of the "measured" inputs of 1 kHz. It can be appreciated that a good match exists between the simulated and estimated variables.

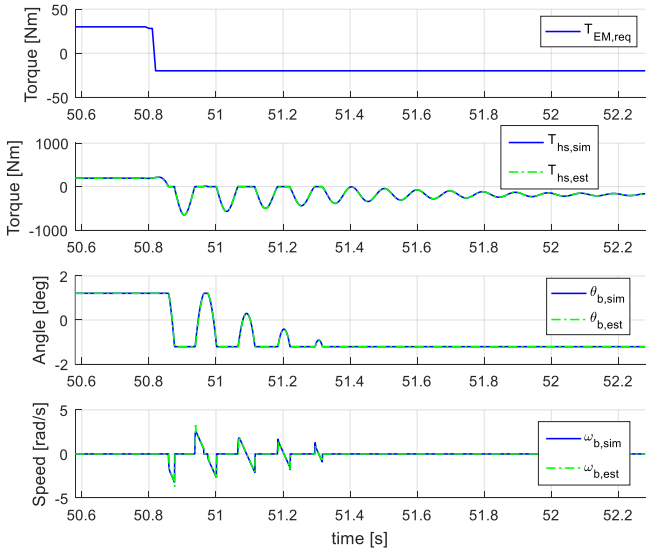


Figure 11. Estimator outputs: mode transition variables.

In Figure 12, the powertrain operating mode is 1 when there is contact on the drive side, 0 when there is no-contact and -1 indicates contact on the coast side. From the backlash position it can be concluded that the mode transitions are promptly detected.

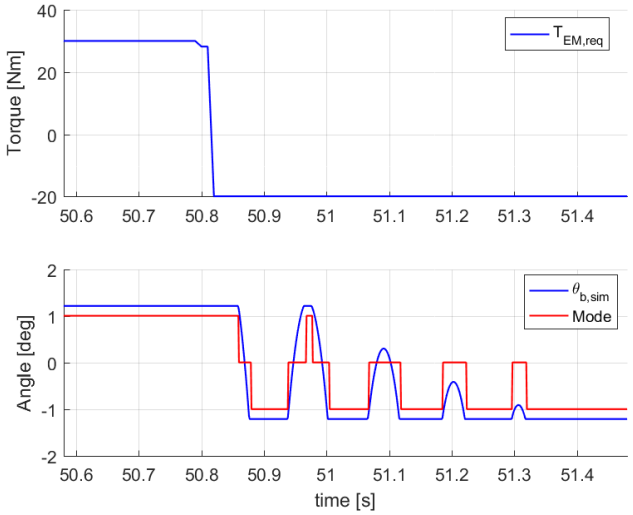


Figure 12. Mode transition verification.

### *Effect of the input sampling frequency*

The effect of the input sampling frequency is assed in this section. Three different values are tested: 100 Hz, 1 kHz and 10 kHz. Respectively, the estimator runs with the following time-steps: 10 ms, 1ms and 0.1 ms.

Figure 13 allows to compare the quality of the estimator outputs obtained for the three tested cases. A delay between the simulated wheel torque and the one computed for the 100 Hz case is clearly seen in the figure. From an implementation point of view, having a lower time resolution on the estimator input with respect to the time-step used for the calculation implies introducing a delay on the estimates. On the other hand, the results obtained for the other two cases are very close to the reference values.

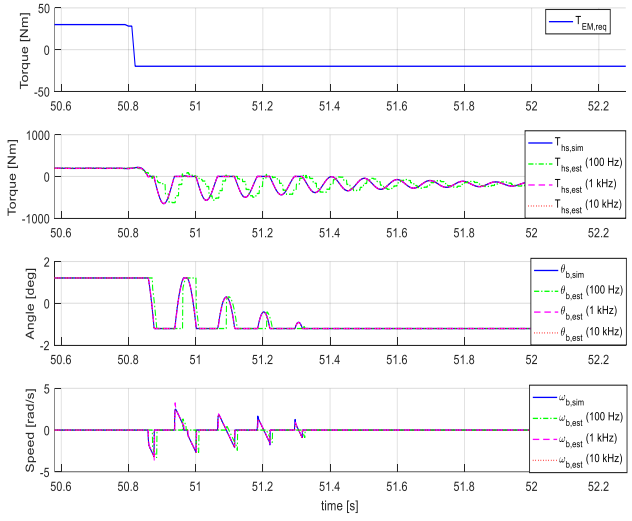


Figure 13. Estimator outputs: mode transition variables for different sampling frequencies.

Figure 14 shows the mode transitions for each of the tested cases. The 100 Hz case presents a considerably higher delay between the indicated powertrain mode and the actual driveline state with respect to the other two cases.

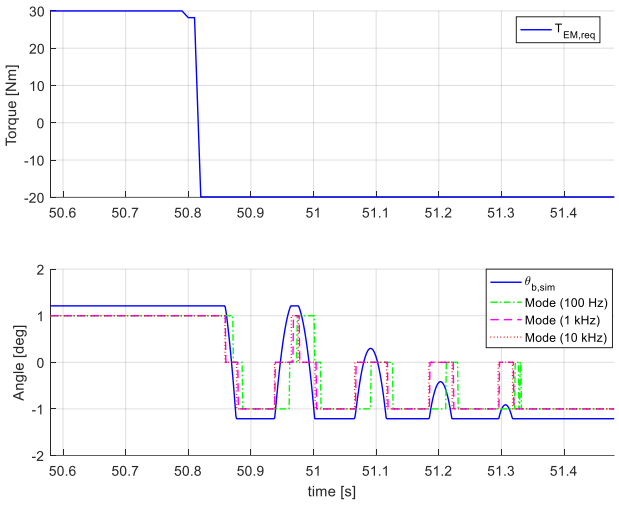


Figure 14. Mode transition verification for different sampling frequencies.

Table 1 presents the delay between the actual time in which the powertrain starts traversing the backlash region after the torque tip-out and the instant in which the mode transition is validated. It can be seen that, with the higher sampling frequencies, the no-contact mode is detected fast enough to significantly anticipate the first impact. On the other hand, with the lowest sampling frequency, the contact loss is detected just 5 ms prior to the re-engagement of the driveline components, given virtually no time for a powertrain control logic to intervene.

Table 1. Mode transition delay.

| Sampling frequency [kHz] | Mode transition delay [ms] |
|---|---|
| 0.1 | 14 |
| 1 | 2 |
| 10 | 0.8 |

## Conclusions

This paper proposes a model-based nonlinear observer that is designed to determine the powertrain operating mode in real-time. The estimator requires as inputs only measurements that are commonly available in passenger cars. The observer is based upon a switching structure that combines a discrete-time Kalman Filter and a control-oriented model of the powertrain.

Due to the faster response of EMs with respect to conventional ICEs and the fact that regenerative braking torque is usually larger than the ICE braking torque in a conventional car, high precision on the system states estimates is required if an observer is meant to be used for drivability control.

A validation of the model was performed using experimental data collected during vehicle testing. The results showed that the model can properly simulate the nonlinear behavior of the powertrain right after tip-in/tip-out events where the impacts within the driveline are more critical for the vehicle dynamic performance.

An assessment on the quality of the predicted state transitions was undertaken and the effect of the sampling frequency was also explored. A value of 1 kHz was found to be high enough for the quality of the estimates to be suitable for control purposes.

Future work will focus on integrating the proposed estimator with powertrain control algorithms aiming at mitigating the negative effects of driveline backlash and shaft flexibility on drivability.

## References


[1] Galvagno, E., Guercioni, G., and Vigliani, A., “Sensitivity Analysis of the Design Parameters of a Dual-Clutch Transmission Focused on NVH performance,” SAE Technical Paper 2016-01-1127, 2016, doi:10.4271/2016-01-1127.

[2] Krenz, R., “Vehicle Response to Throttle Tip-In/Tip-Out,” SAE Technical Paper 850967, 1985, doi:10.4271/850967.

[3] Koprubasi, K., Rizzoni, G., Galvagno, E., Velardocchia, M., “Development and experimental validation of a low-frequency dynamic model for a Hybrid Electric Vehicle”, International journal of powertrains, Vol. 01, no. 03, 2012, pp. 304-333, ISSN: 1742-4267, doi: 10.1504/IJPT.2012.048409.

[4] Lv, C., Zhang, J., Li, Y., Yuan, Y., “Mode-switching-based active control of a powertrain system with non-linear backlash and flexibility for an electric vehicle during regenerative deceleration”, Proceedings of the Institution of Mechanical Engineers, Part D: Journal of Automobile Engineering, Vol. 229, no. 11, 2014, pp. 1429-1442, doi: 10.1177/0954407014563552.

[5] Syed, F.U., Kuang, M.L., Czubay, J., Ying, H., “Derivation and Experimental Validation of a Power-Split Hybrid Electric Vehicle Model”, IEEE Transactions on Vehicular Technology, Vol. 55, no. 06, 2006, pp. 1731-1747, doi: 10.1109/TVT.2006.878563.

[6] Gokdere, L.U., Benlyazid, K., Santi, E., Brice, C.W., Dougal, R.A., “Hybrid electric vehicle with permanent magnet traction motor: A simulation model”, Electric Machines and Drives, 1999. International Conference IEMD '99, Seattle, WA, 1999, pp. 502-504, doi: 10.1109/IEMDC.1999.769158.

[7] Galvagno, E., Morina, D., Sorniotti, A., Velardocchia, M., “Drivability analysis of through-the-road-parallel hybrid vehicles”, Meccanica, Vol. 48, no. 02, 2013, pp. 351-366, ISSN: 0025-6455, doi: 10.1007/s11012-012-9606-6.

[8] Kawamura, H., Ito, K., Karikomi, T., and Kume, T., “Highly-Responsive Acceleration Control for the Nissan LEAF Electric Vehicle,” SAE Technical Paper 2011-01-0397, 2011, doi: 10.4271/2011-01-0397.

[9] Lagerberg, A., Egardt, B., “Backlash Estimation With Application to Automotive Powertrains”, IEEE Transactions on Control Systems Technology, Vol. 15, no. 15, 2007, pp. 483-493, doi: 10.1109/TCST.2007.894643.

[10] Lagerberg, A., “Control and estimation of automotive powertrains with backlash,” Ph.D. dissertation, Dept. Signals Syst., Chalmers Univ. Technol., Göteborg, Sweden, 2004.

[11] Canova, M., Rostiti, C., D'Avico, L., Stockar, S. et all., “Model-Based Wheel Torque and Backlash Estimation for Drivability Control,” *SAE International Journal of Engines* 10(3):2017, doi: 10.4271/2017-01-1111.

[12] Lagerberg, A., Egardt, B., “Backlash gap position estimation in automotive powertrains.” 2003 European Control Conference (ECC), Cambridge, UK, 2003, pp. 2292-2297.

[13] Lagerberg, A., Egardt, B., “Estimation of Backlash in Automotive Powertrains — An Experimental Validation”, IFAC Proceedings Volumes, Vol. 37, no. 22, 2004, pp. 47-52, ISSN: 1474-6670, doi: 10.1016/S1474-6670(17)30320-8.

[14] Templin, P., Egardt, B., “A Powertrain LQR-torque Compensator with Backlash Handling”, Oil & Gas Science and Technology–Revue d’IFP Energies Nouvelles, Vol. 66, no. 04, 2011, pp. 645-654, doi: 10.2516/ogst/2011147.
[15] Templin, P., Egardt, B., “Experimental Results for a Powertrain LQR-torque Compensator with Backlash Handling”, IFAC Proceedings Volumes, Vol. 42, no. 26, 2009, pp. 148-153, ISSN: 1474-6670, ISBN: 9783902661586, doi: 10.3182/20091130-3-FR-4008.00020.
[16] Velardocchia, M., Vigliani, A., “Control systems integration for enhanced vehicle dynamics”, The open mechanical engineering journal, Vol. 07, 2013, pp. 58-69, ISSN: 1874-155X, doi: 10.2174/1874155X01307010058.
[17] Morgando, A., Velardocchia, M., Vigliani, A., Van Leeuven, G.B., Ondrak, V., “An alternative approach to automotive ESC based on measured wheel forces”, Vehicle system dynamics, Vol. 49, no. 12, 2011, pp. 1855-1871, ISSN: 0042-3114, doi: 10.1080/00423114.2010.548526.
[18] Nezhadali, V., Eriksson, L., “Optimal control of engine controlled gearshift for a diesel-electric powertrain with backlash”, IFAC-PapersOnLine, Vol. 49, no. 11, 2016, pp. 762-768, ISSN 2405-8963, doi: 10.1016/j.ifacol.2016.08.111.
[19] Nordin, M., Galic', J., Gutman. P.O., “New models for backlash and gear play”, International journal of adaptive control and signal processing, Vol. 11, no. 01, 1997, pp. 49-63, doi: 10.1002/(SICI)1099-1115(199702)11:1<49::AID-ACS394>3.0.CO;2-X.
[20] Pettersson, M., Nielsen, L., “Gear shifting by engine control”, IEEE Transactions on Control Systems Technology, Vol. 08, no. 03, 2000, pp. 495-507, doi: 10.1109/87.845880.
[21] Templin, P., “Simultaneous estimation of driveline dynamics and backlash size for control design”, 2008 IEEE International Conference on Control Applications, San Antonio, TX, 2008, pp. 13-18, doi: 10.1109/CCA.2008.4629642.
[22] Ferrari-Trecate, G., Mehdi, G., “Observability analysis and state observers for automotive powertrains with backlash: a hybrid system approach”, International Journal of Control, Vol. 79, no. 05, 2006, pp. 496-507, doi: 10.1080/00207170600587507.
[23] Grewal, M.S., Andrews, A.P., “Kalman filtering: Theory and Practice Using MATLAB”, John Wiley & Sons, 2001, ISBN: 0-471-26638-8.

## Contact Information

guido.guercioni@polito.it